

## Video Article

# A High-content Assay for Monitoring AMPA Receptor Trafficking

Mohammad A. Ghane\*<sup>1</sup>, Dina W. Yakout\*<sup>1</sup>, Angela M. Mabb<sup>1</sup><sup>1</sup>Neuroscience Institute, Georgia State University

\*These authors contributed equally

Correspondence to: Angela M. Mabb at [amabb@gsu.edu](mailto:amabb@gsu.edu)URL: <https://www.jove.com/video/59048>DOI: [doi:10.3791/59048](https://doi.org/10.3791/59048)

Keywords: Neuroscience, Issue 143, Trafficking, AMPA, receptor, synapse, plasticity, internalization, endocytosis, exocytosis, Arc, glutamate

Date Published: 1/28/2019

Citation: Ghane, M.A., Yakout, D.W., Mabb, A.M. A High-content Assay for Monitoring AMPA Receptor Trafficking. *J. Vis. Exp.* (143), e59048, doi:10.3791/59048 (2019).

## Abstract

Postsynaptic trafficking of receptors to and from the cell surface is an important mechanism by which neurons modulate their responsiveness to different stimuli. The  $\alpha$ -amino-3-hydroxy-5-methyl-4-isoxazolepropionic acid (AMPA) receptors, which are responsible for fast excitatory synaptic transmission in neurons, are trafficked to and from the postsynaptic surface to dynamically alter neuronal excitability. AMPA receptor trafficking is essential for synaptic plasticity and can be disrupted in neurological disease. However, prevalent approaches for quantifying receptor trafficking ignore entire receptor pools, are overly time- and labor-intensive, or potentially disrupt normal trafficking mechanisms and therefore complicate the interpretation of resulting data. We present a high-content assay for the quantification of both surface and internal AMPA receptor populations in cultured primary hippocampal neurons using dual fluorescent immunolabeling and a near-infrared fluorescent 96-well microplate scanner. This approach facilitates the rapid screening of bulk internalized and surface receptor densities while minimizing sample material. However, our method has limitations in obtaining single-cell resolution or conducting live cell imaging. Finally, this protocol may be amenable to other receptors and different cell types, provided proper adjustments and optimization.

## Video Link

The video component of this article can be found at <https://www.jove.com/video/59048/>

## Introduction

The magnitude and temporal dynamics of neuronal excitability is largely dependent on the availability and composition of surface receptor populations which transduce electrochemical signals. Whereas the synthesis of new receptors (or receptor subunits) is generally an energetically costly and relatively protracted process, a host of cellular machinery dedicated to the endo- and exocytosis of existing receptors provide a means for their fast insertion and removal to and from the membrane<sup>1</sup>. Therefore, in addition to the transcriptional and translational regulation of receptors, posttranslational receptor trafficking is an important modulator of neuronal excitability.

Synaptic plasticity, or the changing strength of connections between neurons with experience, is thought to form the basis of learning and memory<sup>2,3</sup>. The strengthening and weakening of synapses over time, termed long-term potentiation (LTP) and long-term depression (LTD), respectively, can be modulated through the trafficking of  $\alpha$ -amino-3-hydroxy-5-methyl-4-isoxazolepropionic acid (AMPA) receptors<sup>4,5</sup>. AMPA receptors are heterotetramers composed of four subunits (GluA1-4), and mediate the majority of fast excitatory synaptic transmission in the brain<sup>6</sup>. Thus, neuron excitability is in large part a function of the quantity of AMPA receptors at the postsynaptic surface available to be activated by glutamate. LTD is commonly associated with an increase in AMPA receptor endocytosis, whereas LTP is predominantly associated with an increase in AMPA receptor exocytosis. Postsynaptic surface expression of AMPA receptors requires endosomal delivery to exocytotic proteins, where fusion with the plasma membrane then occurs in a calcium-dependent manner<sup>7,8,9,10,11,12,13,14</sup>. There also exist a host of mechanisms that regulate activity-dependent AMPA receptor endocytosis. One example of this is via the immediate early gene *Arc/Arg3.1* (*Arc*). Among other functions<sup>15</sup>, *Arc* is known to mediate metabotropic glutamate receptor (mGluR)-dependent LTD by promoting AMPA receptor endocytosis through its binding partners, which include the endocytic proteins AP-2, endophilin-3, and dynamin-2<sup>16,17,18,19</sup> at clathrin-coated pits<sup>20,21</sup>. Internalized AMPA receptors can either be recycled back to the plasma membrane or earmarked for degradation<sup>22,23</sup>.

Importantly, the subunit composition of AMPA receptors contributes to their trafficking dynamics<sup>24</sup>. Of major relevance is the intracellular C-terminal domain of the subunits, where the majority of posttranslational modifications and trafficking-related protein interactions occur. GluA1 and GluA4 subunit-containing AMPA receptors are particularly apt to being trafficked to the cell surface during LTP, in part due to the presence of their PDZ ligands, ~90 amino acid sequences that promote membrane anchoring via interactions with various PDZ domain-containing proteins<sup>25,26</sup>. On the other hand, AMPA receptors containing GluA2 and lacking GluA1 or GluA4 tend to be trafficked constitutively but accumulate intracellularly with synaptic activity<sup>27</sup>. GluA2 subunits undergo RNA editing which, in addition to promoting retention in the endoplasmic reticulum<sup>28</sup>, renders the channel pore impermeable to calcium<sup>29</sup>, further implicating subunit-specific trafficking as a key mediator of neuronal homeostasis and plasticity. Interestingly, disruption of ubiquitin-dependent *Arc* degradation has been shown to increase GluA1 endocytosis and increase the surface expression of GluA2 subunit-containing AMPA receptors after induction of mGluR-LTD with the selective

group I mGluR agonist (S)-3,5-Dihydroxyphenylglycine (DHPG), indicating that much remains to be learned regarding the mechanisms and role of subunit-specific AMPA receptor trafficking<sup>30</sup>.

Methods for observing changes in surface expression of receptors are often cumbersome, time consuming, or introduce unnecessary confounds. Biotin-based assays are a pervasive and commercially available approach. Affinity purification of biotinylated surface receptors represents one such example, however the necessity of performing electrophoresis requires a large amount of sample material and can render the screening of multiple treatments a prohibitively lengthy process<sup>31</sup>. Extensions of this assay, where multiple time points of labeling and immunoprecipitations are performed to quantify the gradual degradation of an initial signal, similarly neglect the addition of new — or recycled — receptors to the cell surface and only exacerbate the time and material requirements.

Other approaches make use of chimeric constructs or the addition of fluorescent tags to observe receptor trafficking<sup>32</sup>, sometimes using live cell imaging<sup>33,34</sup>. While potentially powerful, these designs can affect the normal trafficking patterns of receptors due to the mutations or dramatic changes in molecular weight introduced in these proteins. The use of dyes that label subcellular compartments by targeting low pH<sup>34,35</sup> are non-specific and make distinguishing between different intracellular compartments important for receptor trafficking (e.g. lysosomes and proteasomes) difficult. Finally, the use of confocal microscopy to visualize the colocalization of receptors with markers associated with trafficking and degradation, such as endosomal proteins or clathrin, while potentially providing useful insight into specific localization with subcellular resolution, are time, labor-intensive, and costly due to the necessity of individually analyzing each cell and the requirement of confocal or super-resolution microscopy.

Here, we demonstrate a high-content receptor trafficking assay that is compatible with primary neuronal culture preparations<sup>30</sup>. This method separately labels the surface and intracellular receptor pools of fixed neurons, enabling the presentation of data as a ratio of normalized surface or internalized receptor density to the overall density for that receptor. The high-content nature of this method is ideal for screening multiple treatments and/or genotypes in a short time frame, and requires only standard cell culturing and antibody incubation expertise.

Briefly, primary neurons are grown in standard 96-well microplates and then treated as dictated by experimental design, incubated with primary antibodies, washed, and fixed. Cells are then incubated with a secondary antibody to label surface receptors, followed by another fixation step. Permeabilization then occurs and a second secondary antibody is used to label internal receptor pools. Finally, cells are imaged using an infrared fluorescent microplate scanner to quantify the integrated density of each receptor population. **Figure 1** summarizes our high-content assay in comparison to a traditional biotinylation assay.

While the protocol offered here is optimized and specific for AMPA receptor trafficking in primary hippocampal neuron cultures, this procedure could, in theory, be extended and adapted for different receptors in a variety of cell types.

## Protocol

All methods described here have been approved by the Institutional Animal Care and Use Committee (IACUC) at Georgia State University.

### 1. Preparation of Primary Hippocampal Neurons (in Laminar Flow Hood)

1. Isolate primary hippocampal neurons from mixed sex postnatal day (P) 0-1 mice as previously described<sup>36</sup>.
2. Plate neurons in 96-well poly-D-lysine coated microplates at a density of  $2 \times 10^4$  cells per well.
3. Prepare media for feeding the neurons by adding 10 mL of 50x B-27, 5 mL of 100x Glutamine, 242  $\mu$ L of 10 mg/mL 5-Fluoro-2'-deoxyuridine (FUDR) and 10  $\mu$ L of 10 mg/mL Gentamycin to 485 mL of neuronal media (see **Table of Materials**).
4. Feed neurons as previously described<sup>36</sup> by removing half (100  $\mu$ L) of the pre-existing media (referred to as conditioned media, which contains constituents that support neuronal survival) from each well and replacing with 100  $\mu$ L of 37 °C prewarmed media prepared in step 1.3 every 3-4 days. Store the conditioned media from each feeding at 4 °C for step 2.3.

### 2. Measuring AMPA Receptor Trafficking in Response to DHPG (in Laminar Flow Hood)

1. At Day In Vitro (DIV) 14, prepare a 500  $\mu$ L stock solution of Tetrodotoxin (TTX) at a concentration of 2 mM using cell culture grade water. **CAUTION:** TTX is a neurotoxin. Handle carefully and avoid contact with skin.
2. Using a multi-channel pipette, remove 100  $\mu$ L from each well of the 96-well microplate of neurons and pool the media.
3. Add 2  $\mu$ L of the TTX stock solution to 1 mL of the pooled conditioned media from step 2.2 to create a 4  $\mu$ M solution of TTX. If there is not enough pooled conditioned media, then use some of the stored conditioned media from Step 1.4.
4. Treat neurons with 100  $\mu$ L/well of the 4  $\mu$ M solution of TTX from step 2.3. Place the microplate in a 5% CO<sub>2</sub> incubator at 37 °C for 4 h.
5. Attach a sterile glass Pasteur pipette to a suction line and attach a sterile 200  $\mu$ L pipette end to the tip of the pipette. Remove the media from each well carefully. Avoid touching the bottom of the microplate where the neurons are located.
6. Add 200  $\mu$ L of room temperature neuronal media to each well.
7. Incubate the microplate at room temperature for 15 min. Incubation in 5% CO<sub>2</sub> is preferred but not necessary.

### 3. Immunolabelling (in Laminar Flow Hood)

1. Prepare a 1:150 dilution of the anti-GluA1 or anti-GluA2 antibody in neuronal media.
2. Remove the neuronal media added in Step 2.6. Add 50  $\mu$ L of the anti-GluA1 or anti-GluA2 antibody solutions to corresponding wells for 20 min at room temperature to allow antibody binding. Add 50  $\mu$ L of neuronal media to the secondary antibody only control wells.
3. Remove the antibody solutions added in step 3.2. Wash the microplate 3 times with 100  $\mu$ L/well room temperature neuronal media to remove any unbound antibodies.

4. Make a 50 mM stock solution of DHPG in neuronal media or cell culture grade water. Vortex the solution briefly to fully dissolve the DHPG. Prepare this solution fresh on the same day of the experiment. Avoid using old or thawed solutions.
5. Dilute the stock solution in neuronal media to 1:500 to make a 100  $\mu$ M solution.
6. Remove the existing media from each well. Add 100  $\mu$ L/well of the 100  $\mu$ M DHPG stock solution from Step 3.5. Incubate the microplate in the incubator at 37 °C in 5% CO<sub>2</sub> for 10 min.
7. Remove the DHPG solution added in step 3.6 and add 100  $\mu$ L/well neuronal media. Repeat this step one more time. Place the microplate in the incubator at 37 °C in 5% CO<sub>2</sub> for 5 min.
8. Add the sucrose to make the 4% paraformaldehyde/4% sucrose solution in PBS on the same day of the experiment. Avoid using old or thawed solutions. Remove the media added in step 3.7. Add 100  $\mu$ L/well of 4% paraformaldehyde/4% sucrose solution. Repeat steps 3.6 – 3.8 for each additional time-point. Once complete, incubate the microplate at 4 °C for 20 min.  
**CAUTION:** Handle paraformaldehyde stocks in a fume hood.
9. Remove fixative from step 3.8 and add 100  $\mu$ L/well of cold 1x DPBS.
10. Remove DPBS. Add 150  $\mu$ L/well blocking buffer (a ready-to-use formulation in TBS, refer to **Table of Materials**) and incubate at room temperature for 90 min. Alternatively, incubate overnight at 4 °C.

#### 4. Labelling Surface Receptors

1. Prepare a 1:1500 dilution of 680RD Goat anti-Mouse IgG secondary antibody in blocking buffer.
2. Remove blocking buffer from step 3.10. Add 50  $\mu$ L/well of the secondary antibody solution and incubate at room temperature for 60 min. Keep the microplate protected from light once the secondary antibodies are added. Make sure to continue to protect the microplate from light during subsequent incubations.
3. Remove the solution from step 4.2. Add 100  $\mu$ L/well TBS (50 mM Tris-HCl, 150 mM NaCl, pH 7.6) and incubate at room temperature for 5 min. Repeat this step 4 additional times.
4. Remove TBS from step 4.3. Add 100  $\mu$ L/well of 4% paraformaldehyde/4% sucrose in PBS and incubate at room temperature for 15 min.
5. Remove solution from step 4.4. Add 100  $\mu$ L/well TBS and incubate at room temperature for 5 min. Repeat this step 2 additional times.

#### 5. Labelling the Internalized Receptor Population

1. Prepare TBS containing 0.2% saponin. Vortex the solution briefly to fully dissolve the saponin powder. Filter the solution using a 0.2  $\mu$ m filter to remove any particles that could cause auto-fluorescence.
2. Add 150  $\mu$ L TBS containing 0.2% saponin and incubate at room temperature for 15 min.
3. Remove saponin solution from step 5.2 and add 150  $\mu$ L/well blocking buffer. Incubate at room temperature for 90 min.
4. Prepare a 1:1500 dilution of 800CW Donkey anti-Mouse IgG secondary antibody in blocking buffer.
5. Remove blocking buffer from step 5.3 and add 50  $\mu$ L/well of the secondary antibody solution. Incubate at room temperature for 60 min.
6. Add 100  $\mu$ L/well TBS and incubate at room temperature for 5 min. Repeat this step 4 additional times.

#### 6. Imaging and Analysis

1. Image the 96-well microplate using an infrared laser imaging system according to manufacturer's instructions. Set the scan resolution to 84  $\mu$ m, the scan quality to medium and the focus offset according to the base height of the 96-well microplate used. Click on the "Image Studio" menu button → Export → Image for Digital Media → Export images at a resolution of 300 dpi, in TIFF format.
2. Download Image J "Fiji" at <https://imagej.net/Fiji/Downloads>
3. Open image in Image J "Fiji". Split color channels by clicking on the "Image" menu Color → Split Channels.
4. Open the ROI manager from "Analyze" → "Tools". Check the box "Labels" in the ROI manager to label the circles with numbers.
5. In the red channel (the 680 nm surface receptor pool), select the Region of Interest (ROI) by selecting the circle tool and drawing a circle that accurately fits the first well. Press Ctrl+T.
6. Drag the circle to the next well and press Ctrl+T. Repeat until all wells are circled.
7. From the ROI manager, click "Measure". Select the values that appear and copy them to a spreadsheet.
8. Click on the green channel (the 800 nm internal receptor pool) and then transpose the selected ROIs from step 6.6 to the image. From the ROI manager, click "Measure". Select the values that appear and copy them to a spreadsheet.
9. Calculate the average integrated density values from the secondary only control wells. Subtract the integrated density values for each experimental well from the average secondary only control integrated density values for the surface receptor pool. Repeat this step for the internal receptor pool.
10. Calculate changes in surface receptor expression using  $R_s/R_t$ , where  $R_s$  represents the integrated density of surface receptors and  $R_t$  represents the integrated density of surface receptors + integrated density of internal receptors.

## Representative Results

Arc/Arg3.1 accelerates AMPA receptor endocytosis through interaction with AP-2, endophilin-3 and dynamin-2<sup>16,18</sup> following mGluR activation<sup>37</sup>. In the Arc knock-in mouse (ArcKR), lysines 268 and 269 in the Arc protein are mutated to arginine, which interferes with Arc ubiquitination. This impairs proteasome-dependent turnover of Arc and prolongs its half-life in neurons<sup>21,30</sup>. In this experiment, the persistence of Arc in regulating AMPA receptor trafficking was examined using the high-content AMPA receptor trafficking assay. Neurons were treated with the Na<sup>+</sup> channel blocker TTX, which inhibits action potentials and reduces Arc levels<sup>38</sup>, followed by DHPG, which induces Arc translation and ubiquitination<sup>37,39</sup>. Both surface and internalized pools of GluA1- (**Figure 2A**) and GluA2-containing (**Figure 3A**) AMPA receptor subunits were measured at 5 and 15 min after DHPG washout. This particular experiment used three technical replicates from 3 independent experiments. ArcKR neurons showed increased GluA1 endocytosis when treated with DHPG compared to WT neurons, an effect that was not seen when neurons were treated with TTX only (**Figure 2B**). Surface expression of GluA2 subunits was significantly increased at short time points compared to WT neurons (**Figure 3B**), indicating a potential subunit replacement<sup>30</sup>. Some wells were treated with secondary antibodies only to control for background fluorescence caused by nonspecific binding.

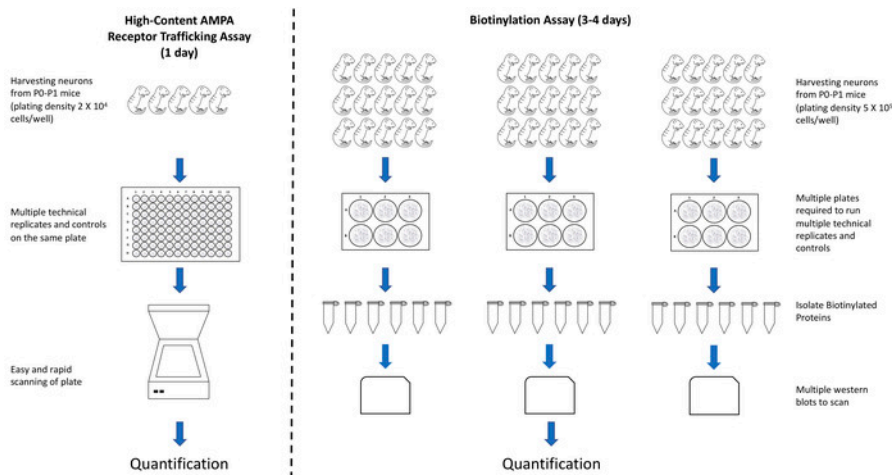


**Figure 1: Comparison of the AMPA receptor high-content trafficking assay to the receptor biotinylation assay.** The high-content trafficking assay consumes less time and resources compared to the standard biotinylation assay. [Please click here to view a larger version of this figure.](#)

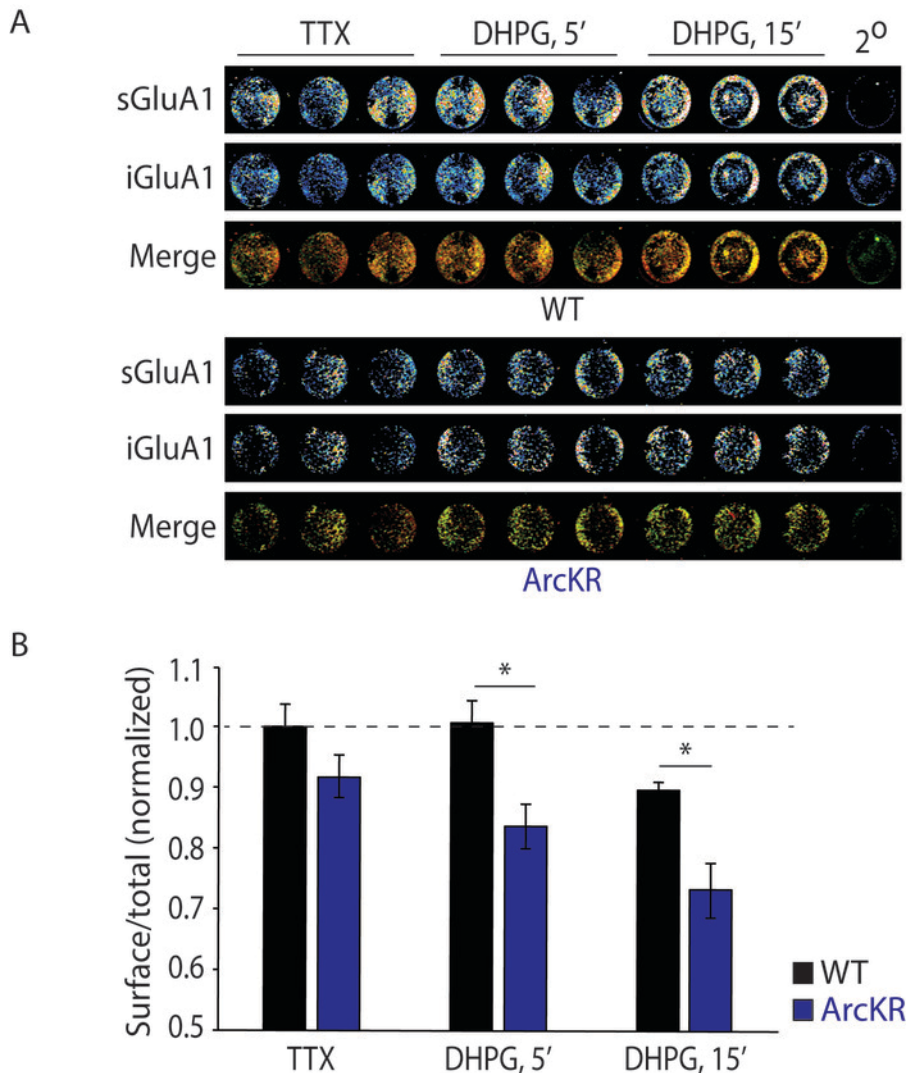


**Figure 2: Surface and internal populations of GluA1 AMPA receptor subunits in WT and ArcKR hippocampal neurons. (A)** Surface (sGluA1) and internalized (iGluA1) GluA1-containing AMPA receptor subunits in WT and ArcKR hippocampal neurons at 5 and 15 min after DHPG washout. Compared to WT, ArcKR neurons have a further decrease in the sGluA1-containing AMPA receptor pool 5 and 15 min after DHPG washout. **(B)** Graph represents surface fluorescence normalized to the total fluorescence intensity. Statistical comparisons were carried out using a one-way ANOVA, paired and unpaired Student's t tests. \* $p \leq 0.05$ ;  $n = 3$  technical replicates from 3 independent experiments. Values represent mean  $\pm$  SEM. This figure has been modified from Wall, M. J. et al. 2018<sup>30</sup>. [Please click here to view a larger version of this figure.](#)

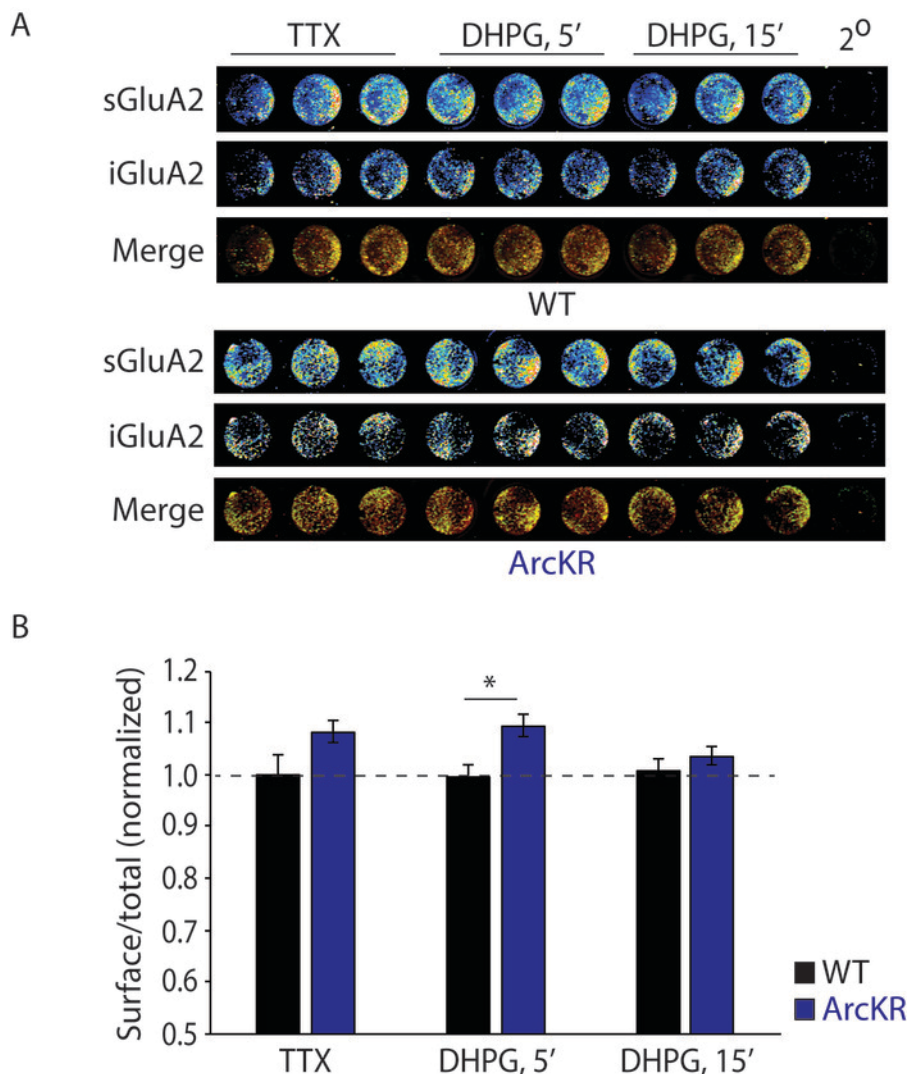


**Figure 3: Surface and internal populations of GluA2 AMPA receptor subunits in WT and ArcKR hippocampal neurons. (A)** The same experimental condition as **Figure 2**. Compared to WT, ArcKR neurons have an increase in the sGluA2-containing AMPA receptor pool 5 min after DHPG washout. **(B)** Graph represents surface fluorescence normalized to the total fluorescence intensity. Statistical comparisons were carried out using one-way ANOVA, paired and unpaired Student's t tests. \* $p \leq 0.05$ ;  $n = 3$  technical replicates from 3 independent experiments. Values represent mean  $\pm$  SEM. This figure has been modified from Wall, M. J. et al. 2018<sup>30</sup>. [Please click here to view a larger version of this figure.](#)

## Discussion

AMPA receptors are an ionotropic glutamate receptor subtype that is integral for neuronal functions which include synapse formation, synapse stability, and synaptic plasticity. AMPA receptor disruption is linked to multiple neurological disorders<sup>24</sup> and are considered attractive drug targets<sup>40</sup>. For example, studies have shown that one of the earliest signs of Alzheimer's disease (AD) is synapse loss and reduced synaptic AMPA receptor levels<sup>41,42</sup>. Intriguingly, addition of Amyloid- $\beta$  oligomers impairs surface GluA1-containing AMPA receptor expression at synapses<sup>43</sup>. Further, status epilepticus down-regulates GluA2 mRNA and protein in hippocampal neurons preceding their death<sup>44</sup>. In amyotrophic lateral sclerosis (ALS), TAR DNA-binding protein (TDP-43) pathology, an ALS-specific molecular abnormality, has been linked to inefficient GluA2 Q/R site-RNA editing<sup>45</sup>.

The high-content AMPA receptor trafficking assay provides an effective means for measuring bulk changes in receptor trafficking profiles within a neuronal network in response to various factors, consuming much less time and materials than alternative methods. A single 96-well microplate provides numerous wells to run multiple technical replicates and controls for different experimental conditions in the same plate. The low plating density of  $2 \times 10^4$  cells/well relative to the  $5 \times 10^5$  cells/well density significantly reduces the number of animals and materials required for each experiment (**Figure 1**). The infrared scanner can image up to six 96-well microplates at a time. The assay can also be modified to a 384-well microplate<sup>46</sup>, which becomes specifically valuable if the assay is run on precious samples that are difficult to obtain or are expensive to culture (e.g. human samples and induced pluripotent stem cells). The entire assay can be completed and analyzed on the same day, which saves valuable time (**Figure 1**).

For successful and efficient completion of the assay, some points need to be considered. First, it is important to prepare the DHPG solution on the same day of neuron treatment. Do not reuse or freeze DHPG stocks. The 4% paraformaldehyde/4% sucrose in PBS solution should

also be made fresh on the same day of the experiment. Second, control wells treated with TTX only or vehicle are required to ensure that the effects observed are specific to treatment. It is also critical to include wells treated with only the secondary antibodies to control for background fluorescence produced by non-specific binding. Note that the second fixation step (following washout of secondary antibodies) is key to reducing secondary antibody background effects and achieving effective labeling of receptor subunits.

Compromises and limitations, as with any method, exist. This assay does not provide single-cell (or subcellular) resolution and does not allow for real-time tracking of receptor trafficking like other methods<sup>32,33,35</sup>. Additionally, proper care must be taken during the permeabilization step of neurons, as this method will be sensitive to the leaking of intracellular components in the case of over-permeabilization.

## Disclosures

The authors have nothing to disclose.

## Acknowledgments

We thank Zachary Allen for technical assistance. This work was supported by the Whitehall Foundation (Grant 2017-05-35) and Cleon C. Arrington Research Initiation Grant Program (RIG-93) to A.M.M. M.A.G. and D.W.Y. were both supported by a Georgia State University Neurogenomics 2CI Fellowship.

## References

- Kennedy, M. J., & Ehlers, M. D. Organelles and trafficking machinery for postsynaptic plasticity. *Annual Review of Neuroscience*. **29** 325-362, (2006).
- Hebb, D. O. *The organization of behavior; a neuropsychological theory*. Wiley (1949).
- Takeuchi, T., Duzsikiewicz, A. J., & Morris, R. G. The synaptic plasticity and memory hypothesis: encoding, storage and persistence. *Philosophical Transactions of the Royal Society London B*. **369** (1633), 20130288, (2014).
- Collingridge, G. L., Isaac, J. T., & Wang, Y. T. Receptor trafficking and synaptic plasticity. *Nature Reviews Neuroscience*. **5** (12), 952-962, (2004).
- Newpher, T. M., & Ehlers, M. D. Glutamate receptor dynamics in dendritic microdomains. *Neuron*. **58** (4), 472-497, (2008).
- Anggono, V., & Huganir, R. L. Regulation of AMPA receptor trafficking and synaptic plasticity. *Current Opinion in Neurobiology*. **22** (3), 461-469, (2012).
- Correia, S. S. *et al.* Motor protein-dependent transport of AMPA receptors into spines during long-term potentiation. *Nature Neuroscience*. **11** (4), 457-466, (2008).
- Wang, Z. *et al.* Myosin Vb mobilizes recycling endosomes and AMPA receptors for postsynaptic plasticity. *Cell*. **135** (3), 535-548, (2008).
- Kennedy, M. J., Davison, I. G., Robinson, C. G., & Ehlers, M. D. Syntaxin-4 defines a domain for activity-dependent exocytosis in dendritic spines. *Cell*. **141** (3), 524-535, (2010).
- Hussain, S., & Davanger, S. Postsynaptic VAMP/Synaptobrevin Facilitates Differential Vesicle Trafficking of GluA1 and GluA2 AMPA Receptor Subunits. *PLoS One*. **10** (10), e0140868, (2015).
- Wu, D. *et al.* Postsynaptic synaptotagmins mediate AMPA receptor exocytosis during LTP. *Nature*. **544** (7650), 316-321, (2017).
- Jurado, S. *et al.* LTP requires a unique postsynaptic SNARE fusion machinery. *Neuron*. **77** (3), 542-558, (2013).
- Arendt, K. L. *et al.* Calcineurin mediates homeostatic synaptic plasticity by regulating retinoic acid synthesis. *Proceedings of the National Academy of Sciences of the United States of America*. **112** (42), E5744-5752, (2015).
- Ahmad, M. *et al.* Postsynaptic complexin controls AMPA receptor exocytosis during LTP. *Neuron*. **73** (2), 260-267, (2012).
- Bramham, C. R., Worley, P. F., Moore, M. J., & Guzowski, J. F. The immediate early gene *arc/arg3.1*: regulation, mechanisms, and function. *The Journal of Neuroscience*. **28** (46), 11760-11767, (2008).
- Chowdhury, S. *et al.* Arc/Arg3.1 interacts with the endocytic machinery to regulate AMPA receptor trafficking. *Neuron*. **52** (3), 445-459, (2006).
- Waung, M. W., & Huber, K. M. Protein translation in synaptic plasticity: mGluR-LTD, Fragile X. *Current Opinion in Neurobiology*. **19** (3), 319-326, (2009).
- Wall, M. J., & Correa, S. A. L. The mechanistic link between Arc/Arg3.1 expression and AMPA receptor endocytosis. *Seminars in Cell and Developmental Biology*. **77** 17-24, (2018).
- DaSilva, L. L. *et al.* Activity-Regulated Cytoskeleton-Associated Protein Controls AMPAR Endocytosis through a Direct Interaction with Clathrin-Adaptor Protein 2. *eNeuro*. **3** (3), (2016).
- Carroll, R. C. *et al.* Dynamin-dependent endocytosis of ionotropic glutamate receptors. *Proceedings of the National Academy of Sciences of the United States of America*. **96** (24), 14112-14117, (1999).
- Mabb, A. M. *et al.* Triad3A regulates synaptic strength by ubiquitination of Arc. *Neuron*. **82** (6), 1299-1316, (2014).
- Ehlers, M. D. Reinsertion or degradation of AMPA receptors determined by activity-dependent endocytic sorting. *Neuron*. **28** (2), 511-525, (2000).
- Petrini, E. M. *et al.* Endocytic trafficking and recycling maintain a pool of mobile surface AMPA receptors required for synaptic potentiation. *Neuron*. **63** (1), 92-105, (2009).
- Henley, J. M., & Wilkinson, K. A. Synaptic AMPA receptor composition in development, plasticity and disease. *Nature Reviews Neuroscience*. **17** (6), 337-350, (2016).
- Hayashi, Y. *et al.* Driving AMPA receptors into synapses by LTP and CaMKII: requirement for GluR1 and PDZ domain interaction. *Science*. **287** (5461), 2262-2267, (2000).
- Sheng, N. *et al.* LTP requires postsynaptic PDZ-domain interactions with glutamate receptor/auxiliary protein complexes. *Proceedings of the National Academy of Sciences of the United States of America*. **115** (15), 3948-3953, (2018).
- Lee, S. H., Simonetta, A., & Sheng, M. Subunit rules governing the sorting of internalized AMPA receptors in hippocampal neurons. *Neuron*. **43** (2), 221-236, (2004).

28. Greger, I. H., Khatri, L., Kong, X., & Ziff, E. B. AMPA receptor tetramerization is mediated by Q/R editing. *Neuron*. **40** (4), 763-774, (2003).
29. Sommer, B., Kohler, M., Sprengel, R., & Seeburg, P. H. RNA editing in brain controls a determinant of ion flow in glutamate-gated channels. *Cell*. **67** (1), 11-19, (1991).
30. Wall, M. J. *et al.* The Temporal Dynamics of Arc Expression Regulate Cognitive Flexibility. *Neuron*. **98** (6), 1124-1132 e1127, (2018).
31. Mammen, A. L., Huganir, R. L., & O'Brien, R. J. Redistribution and stabilization of cell surface glutamate receptors during synapse formation. *The Journal of Neuroscience*. **17** (19), 7351-7358, (1997).
32. Shi, S. H. *et al.* Rapid spine delivery and redistribution of AMPA receptors after synaptic NMDA receptor activation. *Science*. **284** (5421), 1811-1816, (1999).
33. Zhang, Y., Cudmore, R. H., Lin, D. T., Linden, D. J., & Huganir, R. L. Visualization of NMDA receptor-dependent AMPA receptor synaptic plasticity *in vivo*. *Nature Neuroscience*. **18** (3), 402-407, (2015).
34. Hayashi, A., Asanuma, D., Kamiya, M., Urano, Y., & Okabe, S. High affinity receptor labeling based on basic leucine zipper domain peptides conjugated with pH-sensitive fluorescent dye: Visualization of AMPA-type glutamate receptor endocytosis in living neurons. *Neuropharmacology*. **100** 66-75, (2016).
35. Ashby, M. C., Ibaraki, K., & Henley, J. M. It's green outside: tracking cell surface proteins with pH-sensitive GFP. *Trends in Neuroscience*. **27** (5), 257-261, (2004).
36. Correa, S. A., Muller, J., Collingridge, G. L., & Marrion, N. V. Rapid endocytosis provides restricted somatic expression of a K<sup>+</sup> channel in central neurons. *Journal of Cell Science*. **122** (Pt 22), 4186-4194, (2009).
37. Waung, M. W., Pfeiffer, B. E., Nosyreva, E. D., Ronesi, J. A., & Huber, K. M. Rapid translation of Arc/Arg3.1 selectively mediates mGluR-dependent LTD through persistent increases in AMPAR endocytosis rate. *Neuron*. **59** (1), 84-97, (2008).
38. Shepherd, J. D. *et al.* Arc/Arg3.1 mediates homeostatic synaptic scaling of AMPA receptors. *Neuron*. **52** (3), 475-484, (2006).
39. Klein, M. E., Castillo, P. E., & Jordan, B. A. Coordination between Translation and Degradation Regulates Inducibility of mGluR-LTD. *Cell Reports*. (2015).
40. Chang, P. K., Verbich, D., & McKinney, R. A. AMPA receptors as drug targets in neurological disease--advantages, caveats, and future outlook. *European Journal of Neuroscience*. **35** (12), 1908-1916, (2012).
41. Hsieh, H. *et al.* AMPAR removal underlies Abeta-induced synaptic depression and dendritic spine loss. *Neuron*. **52** (5), 831-843, (2006).
42. DeKosky, S. T., & Scheff, S. W. Synapse loss in frontal cortex biopsies in Alzheimer's disease: correlation with cognitive severity. *Annals of Neurology*. **27** (5), 457-464, (1990).
43. Gu, Z., Liu, W., & Yan, Z. {beta}-Amyloid impairs AMPA receptor trafficking and function by reducing Ca<sup>2+</sup>/calmodulin-dependent protein kinase II synaptic distribution. *Journal of Biological Chemistry*. **284** (16), 10639-10649, (2009).
44. Grooms, S. Y., Opitz, T., Bennett, M. V., & Zukin, R. S. Status epilepticus decreases glutamate receptor 2 mRNA and protein expression in hippocampal pyramidal cells before neuronal death. *Proceedings of the National Academy of Sciences of the United States of America*. **97** (7), 3631-3636, (2000).
45. Yamashita, T., & Kwak, S. The molecular link between inefficient GluA2 Q/R site-RNA editing and TDP-43 pathology in motor neurons of sporadic amyotrophic lateral sclerosis patients. *Brain Research*. **1584** 28-38, (2014).
46. Huang, H. S. *et al.* Topoisomerase inhibitors unsilence the dormant allele of Ube3a in neurons. *Nature*. **481** (7380), 185-189, (2011).